COSEIK J. Comput. Struct. Eng., 25(6)
pp.569~577, December, 2012
http://dx.doi.org/10.7734/COSEIK.2012.25.6.569

pISSN 1229-3059 eISSN 2287-2302
Computational Structural
Engineering Institute of Korea

철로의 진동제어를 위한 침목 간격 최적설계

소드빌릭 바트자갈[1] · 카주히사 아베[2†] · 카주히로 고로[1]

[1]니가타대학교 과학기술대학원, [2]니가타대학교 토목건축공학부

Sleeper Spacing Optimization for Vibration Reduction in Rails

Sodbilig Batjargal[1], Kazuhisa Abe[2†] and Kazuhiro Koro[1]

[1]*Graduate School of Science and Technology, Niigata University, Niigata, Japan*
[2]*Department of Civil Engineering and Architecture, Niigata University, Niigata, Japan*

Abstract

In this study, a theoretical investigation of optimized sleeper spacing which can suppress resonances of a railway track is attempted. To achieve this, we introduced a minimization problem in which the objective function is given by the wave transmittance and the design variable is defined by sleeper distribution. In the analysis the rail is modeled by a Timoshenko beam and the sleeper is represented by a mass. The infinite track analysis is realized by attaching the transmitting boundaries at both ends of the finite optimization region. Through numerical analyses the sleeper spacing effective in reduction of the transmittance is discussed. Furthermore, the feasibility of the proposed method is validated in the aspect of vibration reduction through response analyses for a harmonic load.

Keywords : *optimization, sleeper spacing, band structure, vibration reduction*

1. Introduction

The sleeper spacing of railway track has crucial effect on rail vibration properties. Less rail vibration leads to the saving of maintenance cost, safety of railway track and passenger comfort. Therefore, research on the influence of sleeper distribution on the track vibration is significant.

It is known that a railway track has non-uniform sleeper spacing(Wu and Thompson, 2000; Oscarsson, 2002). Wu and Thompson(2000) discussed the stochasticity in sleeper spacing and ballast stiffness. Through numerical experiments they concluded that the pinned-pinned resonance may be suppressed due to the random sleeper spacing. Oscarsson(2002) discussed statistical properties such as rail pad stiffness, ballast stiffness, dynamic ballast-subgrade mass and sleeper spacing. In this work the mean values and standard deviations of these quantities were calculated by perturbation method. However, the first-order statistics was applied only to five-span model. Heckl(1995) investigated the effect of random sleeper spacing on the noise reduction. He concluded that, although the stochasticity in sleeper distance may increase the vibration near the excitation point, it contributes to the reduction of the wave propagation along the rail. Nordborg(1998) has discussed the influence of randomness in the sleeper spacing and pad stiffness on the parametrically excited rail/wheel vibrations. It was found that these irregularities may increase the vibration level under the rail/wheel interaction. In Abe *et al.*(2011), response analyses for a harmonic load have been attempted for uniform and random sleeper spacing railway tracks. As a

† Corresponding author:
E-mail: abe@eng.niigata-u.ac.jp
Received November 19 2012; Revised December 2 2012;
Accepted December 3 2012

result, it was found that the amplitude response of the railway track is less in the latter case. It implies the sleeper spacing affects to the rail vibration. Although, the above mentioned studies focused on tracks with unevenly distributed sleepers, an optimal sleeper distribution for some objective function was not discussed. However, this attempt will contribute to the development of new tracks.

In this study, we theoretically investigate the optimal sleeper spacing which can suppress the resonances of a railway track. In a continuous welded rail, waves propagating in the rail will dominate the dynamic response of track. Especially, the band structure of the track gives some fundamental characteristics of wave modes. Since the resonant frequencies are locating at band edges, excitation of those modes will be avoided by reducing the transmitting energy at the resonant frequencies. Therefore, the optimization problem is defined by minimization of the energy transmittance. The sleeper distribution in a finite track region is considered as design variables. In the analysis numerical model consisting of an infinite rail and discrete sleepers supported on a rigid foundation is considered. Semi-infinite tracks attached at both ends of the optimized region are represented by transmitting boundaries. Through numerical examples the developed optimization method is validated, and the efficiency of the proposed strategy is investigated.

2. Railway Tracking Modeling

Let us consider an infinite track having a finite optimization region subjected to an incident wave u^1 as shown in Figure 1. The track supported by sleepers is rested on a rigid foundation. The left and right semi-infinite periodic tracks have a uniform sleeper spacing l_0. The optimization region consists of n spans in which the sleeper spacing is $l_i (i=1,...,n)$ and the total length is L, i.e.

$$L=\sum_{i}^{n} l_i \tag{1}$$

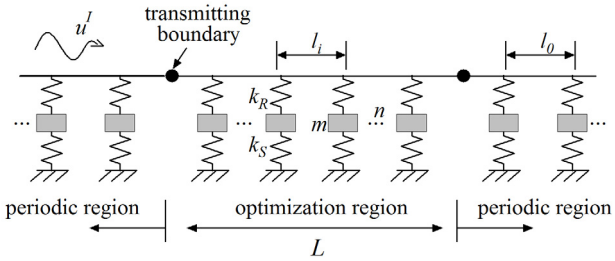

Fig. 1 Infinite railway track

2.1 Equation of Motion of Optimization Region

To achieve the dynamic analysis, the track is divided into three sub-structures as illustrated in Figure 2. $\{F_L\},\{U_L\}$ and $\{F_R\},\{U_R\}$ are internal force and displacement vectors at end nodes of the left and right semi-infinite regions. $\{F_1\},\{U_1\}$ and $\{F_3\},\{U_3\}$ are nodal vectors at both ends of the optimization region. The equation of motion of the optimization region is given by

$$\begin{bmatrix} \widehat{K}_{11} & \widehat{K}_{12} & \widehat{K}_{13} \\ \widehat{K}_{21} & \widehat{K}_{22} & \widehat{K}_{23} \\ \widehat{K}_{31} & \widehat{K}_{32} & \widehat{K}_{33} \end{bmatrix} \begin{Bmatrix} u_1 \\ u_2 \\ u_3 \end{Bmatrix} = \begin{Bmatrix} F_1 \\ 0 \\ F_3 \end{Bmatrix} \tag{2}$$

where $(\ )_2$ is a sub-vector associated with nodes in the optimization region except on the transmitting boundaries. $|\widehat{K}_{ij}|=|\widehat{K}_{ij}-w^2 M_{ij}|$, $|K_{ij}|$ and $|M_{ij}|$ are sitffness and mass sub-matrices, respectively. w is the circular frequency. The external force $\{F_2\}$ acting at the finite region is assumed to be zero. In Equation (2) $\{F_1\}$ and $\{F_3\}$ are given by the following equations(Abe *et al.*, 2012)

$$\{F_1\}=[K_{LR}+K_{LL}]\{u^I\}-[K_{LL}]\{u_1\} \tag{3}$$

$$\{F_3\}=-[K_{RR}]\{u_3\} \tag{4}$$

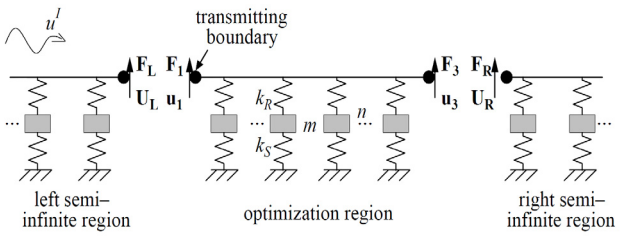

Fig. 2 Sub-structures of railway track

In Equation (3) and (4) $|\boldsymbol{K}_{LR}|$, $|\boldsymbol{K}_{LL}|$, $|\boldsymbol{K}_{RR}|$ are the impedence matrices derived in Abe *et al.*(2012), which represent the semi-infinite regions.

2.2 Solving Equation

Substituting Equation (3) and (4) into Equation (2) and arranging with respect to displacement vector, we can obtain the solving equation:

$$\begin{bmatrix} \widehat{K_{11}}+K_{LL} & \widehat{K_{12}} & \widehat{K_{13}} \\ \widehat{K_{21}} & \widehat{K_{22}} & \widehat{K_{23}} \\ \widehat{K_{31}} & \widehat{K_{32}} & \widehat{K_{33}}+K_{RR} \end{bmatrix} \begin{Bmatrix} u_1 \\ u_2 \\ u_3 \end{Bmatrix} = \begin{Bmatrix} \{K_{LL}+K_{LR}\}u^I \\ 0 \\ 0 \end{Bmatrix} \tag{5}$$

Note that there are no unknowns on the right-hand side. We can thus accomplish the dynamic response analysis. In the optimization analysis the transmittance E_r which is defined by the energy ratio of transmitting wave to incident wave is evaluated. E_r is expressed by

$$E_r = \frac{\overline{E_t}}{\overline{E_i}} \tag{6a}$$

$$\overline{E_i} = \frac{w}{2} Im\left(\left[\overline{u}^I\right]^T [K_{LR}] \{u^I\} \right) \tag{6b}$$

$$\overline{E_t} = \frac{w}{2} Im\left(\left[\overline{u}_3\right]^T [K_{RR}] \{u_3\} \right) \tag{6b}$$

where $\overline{E_i}$ and $\overline{E_t}$ are time averages of the energy of incident and transmitting waves and Im() stands for the imaginary part of a complex number.

3. Optimization Method

3.1 Optimization at a Frequency

Let us consider a minimum transmittance problem for a certain frequency. The objective function J is given by

$$\min_{l_i} J := E_r + \left[\overline{\Lambda}^T\right]\{\tilde{K}U - F\} + \lambda\left(\sum_{i=1}^{n} l_i - L\right) \tag{7}$$

In Equation (7), with the Lagrange multipliers $\{\Lambda\}$ and λ, the following constrained conditions are satisfied

$$|\tilde{\Lambda}^T\{\tilde{K}U - F\} = 0 \tag{8}$$

$$\lambda\left(\sum_{i=1}^{n} l_i - L\right) = 0 \tag{9}$$

where $\{\tilde{K}U - F\} = \{0\}$ is the solving equation of Equation (5). Variation of J due to $l_i \rightarrow l_i + \triangle l_i$ is expressed by

$$\triangle J := \triangle E_r + \left[\tilde{\Lambda}^T\right]\{\triangle \tilde{K}U + \tilde{K}\triangle U\} + \lambda \sum_{i=1}^{n} \triangle l_i \tag{10}$$

Note that, during the optimization process, there is no change in the impedance matrices and thus in the right-hand side of Equation (5) due to the variation of l_i. The variation of the transmittance is given by $\triangle E_r = \triangle \overline{E_i} / \overline{E_i}$. Furthermore, we introduce matrices and as $[K']$ and $[B]$ as

$$\overline{E_t} = \frac{w}{2} Im\left(\left[\overline{U^T}\right][K']\{U\} \right) \tag{11a}$$

$$[K'] = \left[B^T K_{RR} B\right] \tag{11b}$$

$$\{U_3\} = [B]\{U\} \tag{11c}$$

where $[B]$ is a matrix which extracts the component $\{u_3\}$ from the full vector $\{U\}$. Then we obtain the next equation

$$\begin{aligned} \triangle \overline{E_t} &= \frac{w}{2} Im\left(\left[\triangle \overline{U}^T\right][K']\{U\} + \left[\overline{U}^T\right][K']\{\triangle U\} \right) \\ &= \frac{w}{2} Im\left(\left[U^T\right][K'^T]\{\triangle \overline{U}\} + \left[\overline{U^T}\right][K']\{\triangle U\} \right) \end{aligned} \tag{12}$$

In the following, for the sake of simplicity, "Im" will be omitted. For the elimination of $\{\triangle U\}$ and $\{\triangle \overline{U}\}$ in Equation (12), Equation (7) is modified as

$$\begin{aligned} J := E_r &+ \left[\overline{\Lambda_1^T}\right]\{\tilde{K}U - F\} + \left[\overline{U^T}\widetilde{\overline{K}^T} - \overline{F^T}\right]\{\Lambda_2\} \\ &+ \lambda\left(\sum_{i=1}^{n} l_i - L\right) \end{aligned} \tag{13}$$

Then $\triangle J$ is expressed by

$$\triangle J = \frac{w}{2\overline{E_i}} \left(U^T K'^T \triangle \overline{U} + \overline{U^T} K' \triangle U \right) \tag{14}$$

$$+\left[\overline{\Lambda_1^T}\right]\{\triangle\tilde{K}U+\tilde{K}\triangle U\}$$
$$+\left[\triangle\widetilde{U^T}\overline{\tilde{K}^T}+\overline{U^T}\triangle\overline{\tilde{K}^T}\right]\{\Lambda_2\}+\lambda\sum_{i=1}^{n}\triangle l_i$$

From Equation (14), we introduce adjoint problems:

$$[\delta U^T]\left[\tilde{K}^T\right]\{\overline{\Lambda}_1\}=-\frac{w}{2\overline{E_i}}[\delta U^T][K'^T]\{\overline{U}\} \quad (15)$$
$$\left[\delta\tilde{U}^T\right]\left[\overline{\tilde{K}}^T\right]\{\Lambda_2\}=-\frac{w}{2\overline{E_i}}\left[\delta\overline{U}^T\right][K']\{U\}$$
for $\forall\{\delta U\}$

Equation (15) leads to the following equation:

$$\left[\tilde{K}^T\right]\{\overline{\Lambda}_1\}=-\frac{w}{2\overline{E_i}}[K'^T]\{\overline{U}\} \quad (16)$$
$$\left[\tilde{K}^T\right]\{\overline{\Lambda}_2\}=-\frac{w}{2\overline{E_i}}[\overline{K}']\{\overline{U}\}$$

Substituting Equation (16) into Equation (14), we obtain the design sensitivity:

$$\triangle J=\left[\overline{\Lambda}_1^T\right][\triangle\tilde{K}]\{U\}+\left[\Lambda_2^T\right]\left[\triangle\overline{\tilde{K}}\right]\{\overline{U}\}+\lambda\sum_{i=1}^{n}\triangle l_i \quad (17)$$

Since $|\triangle\tilde{K}|=|\triangle\hat{K}|$ and $|\hat{K}|$ is a real matrix, the next relation can thus be obtained

$$\triangle J=\left[\overline{\Lambda}_1^T\right][\triangle\tilde{K}]\{U\}+\left[\Lambda_2^T\right]\left[\triangle\overline{\tilde{K}}\right]\{\overline{U}\}+\lambda\sum_{i=1}^{n}\triangle l_i \quad (18)$$
$$=\left[\overline{\Lambda}_1^T\frac{\partial\hat{K}U}{\partial I}+\Lambda_2^T\frac{\partial\hat{K}\overline{U}}{\partial I}+\lambda\mathbf{1}\right]\{\triangle\mathbf{1}\}$$
$$:=[\beta+\lambda\mathbf{1}]\{\triangle\mathbf{1}\}$$

where $[\mathbf{1}]$ is a row vector consisting of the same component of 1, and $\{\triangle\mathbf{1}\}=\{l_1,l_2,\cdots,l_n,\}$. In order to assure the improvement, $\{\triangle\mathbf{1}\}$ is given by

$$\{\triangle\mathbf{1}\}=-\{\beta+\lambda\mathbf{1}\}\triangle t \quad (19)$$

In Equation (19), $\triangle t>0$ controls the maximum increment of sleeper spacing per optimization step. Substituting Equation (19) into Equation (18), we obtain

$$\triangle J=[\beta+\lambda\mathbf{1}]\{\triangle\mathbf{1}\}=-\parallel\beta+\lambda\mathbf{1}\parallel^2\triangle t<0 \quad (20)$$

Note that $\triangle J<0$ is guaranteed from Equation (20) and thus the minimum value of J will be obtained in a process of the optimization.

Also, the following condition is needed to satisfy the restriction condition of Equation (1),

$$\sum_{i=1}^{n}\triangle l_i=-\triangle t\left(\sum_{i=1}^{n}\beta_i+n\lambda\right)=0 \quad (21)$$

Therefore λ can be determined as

$$\lambda=-\frac{1}{n}\sum_{i=1}^{n}\beta_i \quad (22)$$

3.2 Optimization Under a Frequency Range

In the prior subsection the objective function is evaluated at a certain frequency. However, it is practical to discuss the performance in a range of frequency band. For this purpose, let us recast the minimization problem as

$$J:=\int_{\Omega}^{a}\left(E+\left[\overline{\Lambda_1^T}\right]\{\tilde{K}U-F\}+\left[\widetilde{U^T}\overline{\tilde{K}^T}-\overline{F^T}\right]\{\Lambda_2\}\right)dw \quad (23)$$
$$+\lambda\left(\sum_{i=1}^{n}l_i-L\right)$$

where Ω stand for target frequency bands. The similar procedure to the above formulation leads to the design sensitivity:

$$\triangle J=\left[\int_{\Omega}\left(\overline{\Lambda}_1^T\frac{\partial\hat{K}}{\partial\mathbf{1}}U+\Lambda_2^T\frac{\partial\hat{K}}{\partial\mathbf{1}}\overline{U}\right)dw+\lambda\mathbf{1}\right]\{\triangle\mathbf{1}\} \quad (24)$$
$$:=[B+\lambda\mathbf{1}]\{\triangle\mathbf{1}\}$$

In the following examples, the optimized sleeper spacing is obtained from Equation (24).

4. Numerical Examples

4.1 Optimization Analysis

4.1.1 Optimal Sleeper Arrangement

The track consists of an infinite rail of JIS 50kgN and sleepers of 100kg per one rail. The values of pad stiffness are k_R=110MN/m and k_S =30MN/m. In the analysis the rail is modeled by a Timoshenko beam and the sleeper is represented by a mass. The rail in a unit cell is divided into 12 beam elements. The transmitting boundaries are attached at both ends of the optimization region. The number of spans in the region are 9(n=9) and the initial sleeper spacing is constantly 60cm(l_i =60cm). The sleeper spacing of the right and left semi-infinite regions is also 60cm(l_0=60cm). The allowable maximum increment of the sleeper spacing per optimization step is 0.5cm. Also, the maximum and minimum values of sleeper spacing are limited by 65cm and 55cm respectively.

The band structure of a periodic system can be obtained by dispersion analysis(Mead, 1970). Figure 3 shows the dispersion curves for a periodic track in which the sleeper spacing is constantly 60cm(l_i =60cm). A frequency range in which a dispersion curve is lying is called pass band, while other one is called stop band. It is known that resonance occurs at the band edges, i.e. at 76Hz, 173Hz, 343Hz, 942Hz and 1036Hz. As given in Equation (19) the transmittance is evaluated by an incident wave. Therefore, the transmittance can be calculated only for frequencies whereat the propagating modes exist.

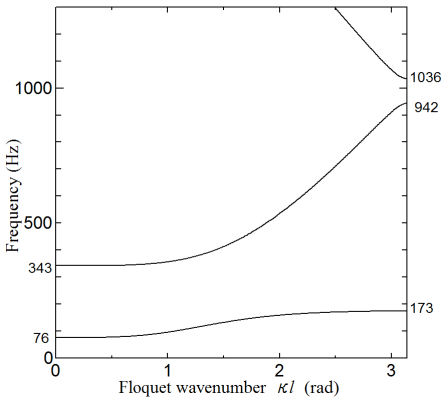

Fig. 3 Dispersion curves of track with uniform sleeper spacing(l=60cm)

The transmittance of the uniform sleeper spacing case is shown in Figure 4. Frequency bands of E_r =1 is the pass band, while E_r=0 is the stop band. Since resonance occurs at the band edges, reduction

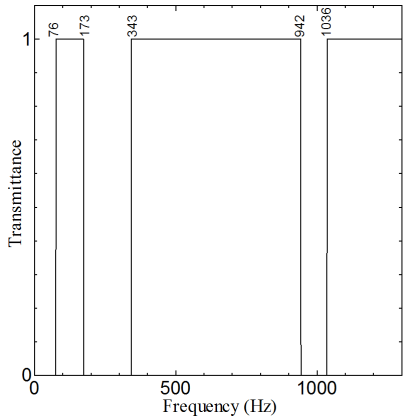

Fig. 4 Transmittance of track with uniform sleeper spacing(l=60cm)

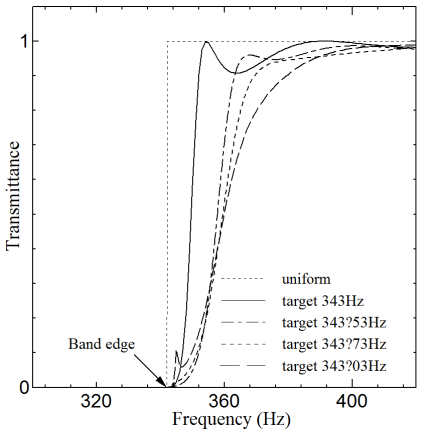

Fig. 5 Transmittance of optimized tracks with target frequencies around 343Hz

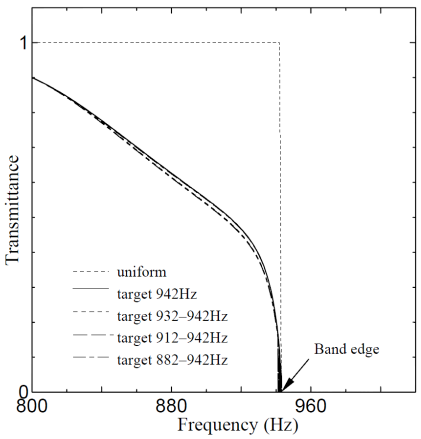

Fig. 6 Transmittance of optimized tracks with target frequencies around 942Hz

of the transmittance around the band edges is investigated. Numerical results for several target band ranges near the resonant frequencies of 343Hz and 942Hz are shown in Figure 5 and 6, respectively. Results for simultaneous optimization for both bands are also shown in Figure 7. From these figures it is found that the optimization of sleeper spacing is effective in reducing the transmittance of high-frequency band, particularly.

As will be shown in the later, the optimized sleeper spacing effective in reducing the transmittance at the high-frequency band is consisted of span length of 55cm, 60cm and 65cm. The dispersion curves of tracks with different uniform sleeper spacing cases of =65cm, 60cm and 55cm are shown in Figure 8. From the figure it can be found that the dependency of the band structure on the sleeper spacing is increased with increasing frequency. The stop bands at the higher frequency for each case are in the range of 829~924Hz, 942~1036Hz and 1082~1168Hz, respectively. Thus, we can realize that this change of the band structures broaden the stop band and results in the reduction of energy transmittance in the wide high-frequency range of 800~1200Hz.

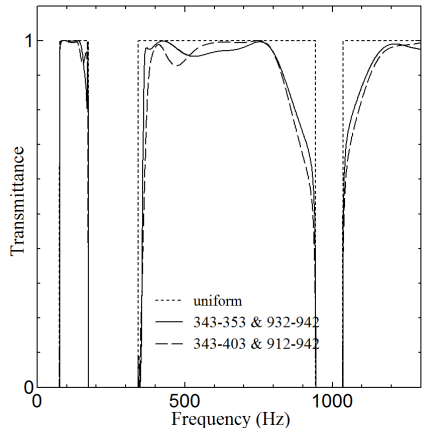

Fig. 7 Transmittance of optimized track with target frequencies around 343Hz and 942Hz

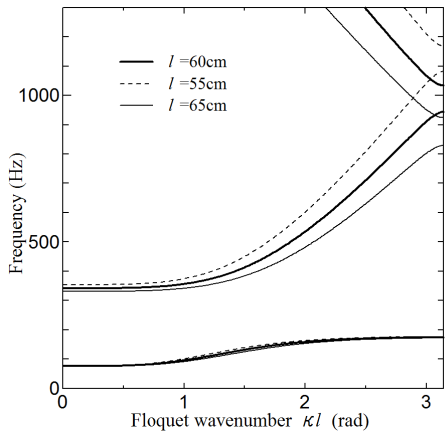

Fig. 8 Dispersion curves of track with different sleeper spacing

4.1.2 Influence of the Number of Spans on Optimization

We evaluate the influence of the number of spans on the optimization process. Numerical results are summarized in Table 1 for target band around 942Hz. The transmittance obtained for the optimi-

Table 1 Optimized sleeper spacing for different number of spans(cm)

Span No	$n=9$	$n=10$	$n=13$	$n=16$
1	55	55	55	55
2	55	55	55	55
3	55	55	55	55
4	55	55	55	55
5	60	55	55	55
6	65	65	55	55
7	65	65	60	55
8	65	65	65	65
9	65	65	65	65
10		65	65	65
11			65	65
12			65	65
13			65	65
14				65
15				65
16				65

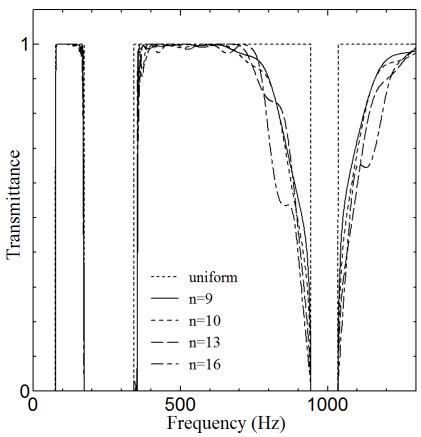

Fig. 9 Influence of the number of spans on performance

zations in the table is shown in Figure 9. It can be observed that the reduction of transmittance near 942Hz has been achieved even for the small number of spans.

Therefore, it can be concluded that nine spans are enough to activate the optimization. It means that the rather small number of spans =9 can reproduce the band structure shown in Figure 8.

4.1.3 Influence of Initial Value of Sleeper Spacing on Optimization

In the above the initial sleeper spacing was fixed to 60cm. In the following analysis, unevenly distributed initial sleeper spacing is considered. Two types of initial sleeper spacing are employed, i.e. a narrowly varied(Case 1) and a widely varied(Case 2) arrangements. In both cases the optimization is achieved for the target band of 932~942Hz.

The sleeper spacing before and after the optimization is listed in Table 2. Both cases result in the same optimized sleeper spacing as the constant initial sleeper spacing case. Therefore, it can be found that setting of the initial value of sleeper spacing does not affect the optimization.

Table 2 Optimized sleeper spacing for different initial values(cm)

Span No	case 1 (before)	case 1 (optimized)	case 2 (before)	case 2 (optimized)
1	60.2	65.0	65.0	65.0
2	60.3	65.0	62.0	65.0
3	60.4	65.0	61.0	65.0
4	60.5	65.0	61.0	65.0
5	59.5	60.0	59.0	60.0
6	59.6	55.0	57.0	55.0
7	59.7	55.0	55.0	55.0
8	59.8	55.0	59.0	55.0
9	59.9	55.0	60.0	55.0

4.2 Harmonic Loading of Railway Track

4.2.1 Analytical Conditions

To verify the feasibility of the proposed method, the optimized sleeper spacing railway track subjected to a harmonic load is analyzed. In order to obtain the vibration characteristics same as the actual railway track, sufficient length is set in the track model. The track model consists of 40(N=40) units of the optimized region consisting of 9 spans, i.e. the total length is 216m. In order to introduce the damping in the track, the pads are given by complex stiffness as

$$k'_R = k_R(1+iwg) \qquad (24)$$
$$k'_S = k_S(1+iwg)$$

where $i=\sqrt{-1}$, and g is damping coefficient. In the following analysis, g=0.0001. Harmonic loading is located at the center of a span of the middle unit. The analytical conditions are illustrated in Figure 10 and 11.

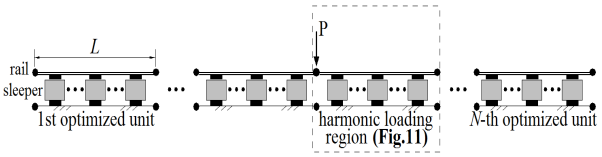

Fig. 10 Finite track model consisting of optimized regions

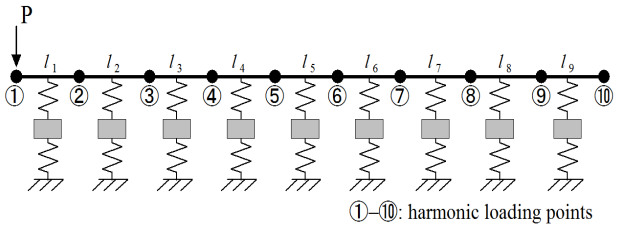

Fig. 11 Harmonic loading region

4.2.2 Numerical Results

Three types of sleeper spacing are employed, i.e uniform(l_i=60cm), optimized(listed in Table 2) and random distributions in the range of $55 \leqq l_i \leqq 65$cm. As a result the receptance at the loading points ②-④, ⑤-⑥ and ⑦-⑨ are in same tendency of characteristics, respectively. Also, due to the symmetry of the repetition pattern, dynamic reaction at points ① and ⑩ are resulted completely same. Therefore, numerical results of loading at points ①, ③, ⑤ and ⑧ are shown in Figure 12. In the uniform sleeper spacing case resonance is sharply outstanding at about 1000Hz for all of the loading points. In the

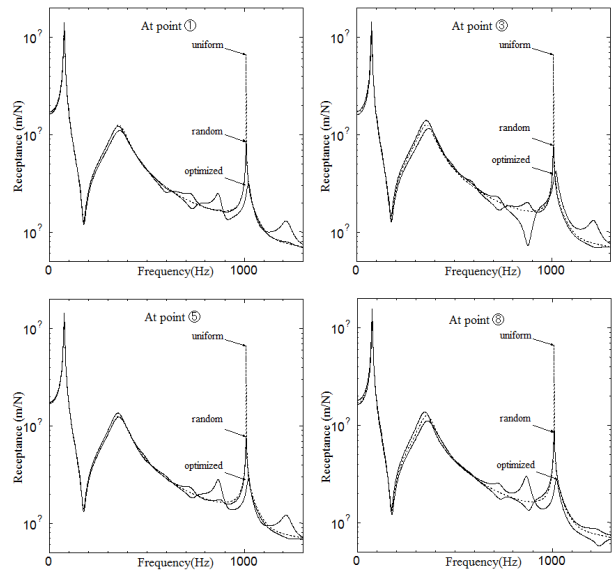

Fig. 12 Influence of sleeper distribution on dynamic reaction

case of random sleeper spacing the resonance around 1000Hz is smaller than the uniform one. However, rather large outstanding resonance is still observed. Contrary to this, the optimized sleeper spacing case has much less sharp resonance in the vicinity of 1000Hz irrespective of the position of loading point. It can be concluded that the employment of the optimized sleeper spacing region leads to less vibration in the rail model. Wave length of rail modes becomes comparable with the sleeper spacing at 500Hz or higher. Thus, the optimization of sleeper distribution will be effective for these higher frequencies. As mentioned above, this fact can be realized by the dependency of dispersion curves on the sleeper spacing shown in Figure 8.

5. Conclusions

In this paper, we have developed an optimization method in which the objective function is given by the transmittance and the design variable is defined by the sleeper distribution. Through numerical analyses it was found that the optimization of sleeper spacing is particularly effective in reducing the transmittance of high-frequency bands. Furthermore, the feasibility of the proposed method was validated through response analyses for a harmonic load. The optimization of sleeper spacing will be effective to suppress the resonance at higher band edges.

Since the wave length of rail modes becomes comparable with the sleeper distance at about 500Hz or higher, the optimization of sleeper distribution will be effective for these higher frequencies. On the one hand, the resonance at a frequency lower than 100Hz is dominated by the sleeper vibration. Hence it is difficult to reduce this resonant peak by controlling the sleeper spacing. Instead of this method, the employment of low stiffness pads will be more effective at lower frequencies. Therefore, it can be concluded that the combination of the conventional means with the proposed optimization of sleeper position will be desirable for the comprehensive vibration reduction of the railway tracks.

Acknowledgment

This work was supported by JSPS KAKENHI Grant No.24560578.

References

Abe, K., Kikuchi, A., Koro, K. (2012) Wave Propagation in an Infinite Track Having an Irregular Region, Noise and Vibr. Mitigation of Rail Trans. Sys., Notes on Num. Fluid Mech. Multidisc. Design, 118, T.Maeda *et al*.(eds), pp.71~79, Springer.

Abe, K., Shimizu, S., Aikawa, A., Koro,K. (2011) Theoretical Study on a Measuring Method of Rail Axial Stress via Vibration Modes of Periodic Track, Proceedings of WCRR 2011.

Heckl, M.A. (1995) Railway Noise-Can Random Sleeper Spacing Help?, ACUSTICA, 81, pp.559~564.

Mead, D.J. (1970) Free Wave Propagation in Periodically Supported Infinite Beams, *Journal of Sound and Vibration*, 11, pp.181~197.

Nordborg, A. (1998) Parametrically Excited Rail/Wheel Vibrations Due to Track Support Irregularities, *ACUSTICA*, 84, pp.854~859.

Oscarsson, J. (2002) Dynamic Train-Track Interaction: Variability Attributable to Scatter in the Track Properties, *Veh, Sys. Dyn*, 37(1), pp.59~79.

Wu, T.X., Thompson, D.J. (2000) The Influence of Random Sleeper Spacing and Ballast Stiffness on the Vibration Behaviour of Railway Track, *ACUSTICA*, 86, pp.313~321.

요 지

본 연구에서는, 철로(railway track)의 공명현상을 제어할 수 있는 침목(sleeper) 간격의 최적화에 대한 이론적 고찰을 소개한다. 이러한 현상을 제어하기 위해 목적함수가 파동 투과율(wave transmittance) 그리고 설계변수가 침목 분포인 최소화 문제를 제안한다. 해석에서 철제 궤도(rail)은 티모센코(Timoshenko) 빔, 침목은 질량으로 표현하였다. 무한 철로는 유한한 최적설계 영역의 양 끝단에 투과경계조건(transmitting boundary)를 부여함으로써 구현하였다. 수치예제를 통하여 침목의 간격에 따른 투과율의 감소의 효과를 살펴보았다. 또한, 하모닉(harmonic) 하중 하에서 응답해석을 통한 진동의 제어 관점에서 제안된 방법의 적합성을 보였다.

핵심용어 : 최적화 설계, 침목간격 설계, 밴드구조, 진동제어